SCIENCE CHINA
Chemistry

• ARTICLES •

March 2016 Vol.59 No.3: 360–369
doi: 10.1007/s11426-015-5508-5

CO_2 solubility in aqueous solutions of *N*-methyldiethanolamine+piperazine by electrolyte NRTL model

Jicai Huang[1,2], Maoqiong Gong[1*], Xueqiang Dong[1], Xiaodong Li[3] & Jianfeng Wu[1]

[1]*Technical Institute of Physics and Chemistry, Chinese Academy of Sciences, Beijing 100190, China*
[2]*University of Chinese Academy of Sciences, Beijing 100049, China*
[3]*School of Energy and Power Engineering, Beihang University, Beijing 100191, China*

Received May 30, 2015; accepted August 7, 2015; published online November 16, 2015

Accurate modeling of the solubility behavior of CO_2 in the aqueous alkanolamine solutions is important to design and optimization of equipment and process. In this work, the thermodynamics of CO_2 in aqueous solution of *N*-methyldiethanolamine (MDEA) and piperazine (PZ) is studied by the electrolyte non-random two liquids (NRTL) model. The chemical equilibrium constants are calculated from the free Gibbs energy of formation, and the Henry's constants of CO_2 in MDEA and PZ are regressed to revise the value in the pure water. New experimental data from literatures are added to the regression process. Therefore, this model should provide a comprehensive thermodynamic representation for the quaternary system with broader ranges and more accurate predictions than previous work. Model results are compared to the experimental vapor-liquid equilibrium (VLE), speciation and heat of absorption data, which show that the model can predict the experimental data with reasonable accuracy.

***N*-methyldiethanolamine, piperazine, carbon dioxide, electrolyte NRTL**

Citation: Huang JC, Gong MQ, Dong XQ, Li XD, Wu JF. CO_2 solubility in aqueous solutions of *N*-methyldiethanolamine+piperazine by electrolyte NRTL model. *Sci China Chem*, 2016, 59: 360–369, doi: 10.1007/s11426-015-5508-5

1 Introduction

Aqueous solutions of alkanolamines are widely used to remove sour gases, such as hydrogen sulfide and carbon dioxide, from natural gas or gaseous effluent by chemical absorption. One of the most commonly used chemical absorbents is activated *N*-methyldiethanolamine (MDEA) [1,2], and piperazine (PZ) is considered as an effective activator for the CO_2 removal process [1]. Design and optimization of the gas-treating process require knowledge of the solubility behavior. However, unlike the physical absorption and desorption processes, the treating processes involve vapor-liquid and chemical reaction equilibriums. Furthermore, the absorption occurs at elevated pressure and low temperature while the desorption takes place at low pressure and elevated temperature. Therefore, the solubility behavior should be studied within relatively wide ranges of temperature, pressure, amine and sour gas concentration. Due to the existence of the two kinds of equilibriums which results in a number of speciation including molecules and ions, it is difficult to develop a thermodynamic model to accurately describe the properties of aqueous electrolyte solutions. Design and optimization of the process had been hindered, and were mainly based on empirical method for a long time.

Since a large number of experimental solubility data of sour gases have been available in the literature, correlation and prediction of these data with an appropriate model is the objective. Kent and Eisenberg [3] used a simple model to correlate the solubility of sour gases in amine solutions.

*Corresponding author (email: gongmq@mail.ipc.ac.cn)

They employed apparent equilibrium constants which are related to component concentrations rather than activities in the equations of chemical equilibriums. Although many people [4–6] adopted the simple model or its modified forms to represent the experimental data, the method has two significant drawbacks [7]. First, the method cannot be confidently extended to the range which is not used to adjust the equilibrium constants. Second, the true compositions of molecules and ions in liquid phase are not available resulting from the lack of accurate activity coefficients of the speciation. Hence, it is necessary to develop a more rigorous thermodynamic model to correlate and predict the experimental data. There are two methods to study the electrolyte solutions. The first one is equation of state. Li and Fürst [8] adopted the electrolyte equation of state to study the solubility of H_2S and CO_2 in aqueous MDEA solution. Derks *et al*. [9] used the model to describe the thermodynamics of H_2O-PZ-MDEA-CO_2 which neglected the presence of carbonate ions and only considered the interactions between cations and anions, and cations and molecular speciation. The model predicted the limited experimental data with reasonable accuracy. The second method is the activity coefficient model based on excess Gibbs free energy which is more widely used.

Deshmukh and Mather [10], Liu *et al*. [1], Vahidi *et al*. [11], and Najibi and Maleki [12] studied the solubility of CO_2 in aqueous solution of MDEA and PZ employing extended Debye-Huckel model for the excess Gibbs free energy. The correlation and prediction results can accurately represent the experimental data in their study range. However, the comparisons of model results with other experimental data were insufficient. Pérez-Salado Kamps *et al*. [13], Bottger *et al*. [14], Speyer *et al*. [15], and Ermatchkov and Maurer [16] investigated the solubility of CO_2 in aqueous solution of PZ activated MDEA using Pitzer equation for calculating the activity coefficients. Model results were widely compared to the experimental data that are available in the literatures. The correlation and prediction results agreed well with many experimental data. Nevertheless, there were still part of the data that cannot be predicted accurately. Apart from the extended Debye-Huckel and Pitzer models, the electrolyte non-random two liquids (NRTL) model was also used in the system. Bishnoi [17] investigated the thermodynamics of H_2O-PZ-MDEA-CO_2 using electrolyte NRTL model. Model results only agreed well with limited experimental data, and the extrapolation was poor. Pinto *et al*. [18] also studied the thermodynamics of the quaternary system by the method, and a total of 312 parameters were regressed to the system. Although a large number of parameters were fitted, model results did not agree well with experimental data in the low pressure region.

Aqueous solution of PZ and MDEA are widely used in the gas-treating process, but none of the models can accurately represent all the experimental data available in the literature. Since the amine-water system is more properly treated as a mixed solvent system instead of a single solvent system that Pitzer equation deals with [7], in the study, the thermodynamics of H_2O-PZ-MDEA-CO_2 is studied by the electrolyte NRTL model. The objective of this work is to try to accurately represent experimental data in a wide range and with relatively few interaction parameters. Unlike the previous studies [16–18], the chemical equilibrium constants are not defined as temperature dependent functions, but rather calculated from standard Gibbs free energy of formation which is regressed to the experimental data. Simultaneously, the Henry's constants of CO_2 in the PZ and MDEA are regressed to revise the value in the pure water. The method increases the degree of freedom of temperature dependent chemical equilibrium constants and Henry's constant in pure water which is beneficial to accurately describe the solubility behavior in different temperature conditions. Furthermore, many new data for thermodynamics of the system and subsystems have been available in recent years which cover wider ranges of temperature, pressure, amine and CO_2 concentrations. These data are either added to the regression process or compared to the predicted results. Therefore, this model should provide a comprehensive thermodynamic representation for the quaternary system with broader ranges and more accurate predictions than previous work [17,18]. To test the model, predicted results are compared to experimental vapor-liquid equilibrium (VLE), speciation and heat of absorption data.

2 Thermodynamic model

2.1 Chemical and vapor-liquid equilibriums

Figure 1 shows the vapor-liquid equilibrium and chemical reactions in aqueous solution of PZ, MDEA and CO_2. In the liquid phase, there are the following reactions: the dissociation of water (R1), the formation and dissociation of bicarbonate (R2, R3), the protonation of MDEA (R4), the protonation and diprotonation of PZ (R5, R6), and the formation of PZ carbamate, PZ dicabamate and protonated PZ carbamate (R7–R9). Due to the existence of chemical reactions, carbon dioxide dissolves in liquid phase not only in molecular form, but also in nonvolatile ionic form. The condition for chemical equilibrium yields the following equation for a reaction *j*:

$$K_j = \prod_i a_i^{\nu_{i,j}} = \prod_i (x_i \gamma_i)^{\nu_{i,j}} \tag{1}$$

The chemical equilibrium constant is given by [19]:

$$\begin{aligned} -\ln K_j &= \frac{\Delta_r G_m^\theta}{RT} = \frac{\Delta_r G_{0,m}^\theta - \Delta_r H_{0,m}^\theta}{RT_0} \\ &+ \frac{\Delta_r H_{0,m}^\theta}{RT} + \frac{1}{RT}\int_{T_0}^{T} \Delta_r C_{p,m}^\theta \mathrm{d}T - \int_{T_0}^{T} \frac{\Delta_r C_{p,m}^\theta}{RT} \mathrm{d}T \end{aligned} \tag{2}$$

The standard property changes of reaction (Gibbs free

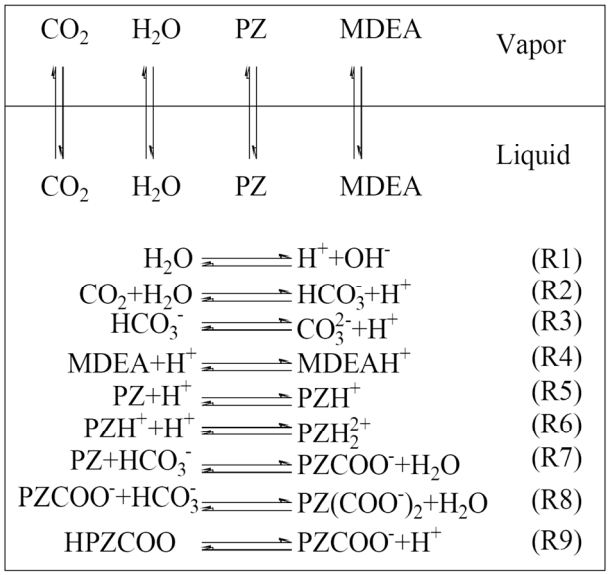

Figure 1 VLE and chemical reactions in the H_2O-PZ-MDEA-CO_2.

energy, enthalpy and heat capacity) are defined as the difference between the standard property of the product and reactant, weighted by their stoichiometric coefficients.

$$\Delta_r M^{\theta} = \sum_i \nu_i M_i^{\theta} \tag{3}$$

To use Eq. (2), the parameters such as Gibbs free energy of formation, enthalpy of formation and coefficients for the temperature dependent heat capacity of speciation are determined by simultaneous regression of the binary interaction parameters. By the method, the relationship of chemical equilibrium constants and temperature is translated to the temperature dependence of these properties which increases the degree of freedom, and is beneficial to describe the solubility behavior in different temperature conditions. Besides, the method maintains thermodynamic consistency between speciation and properties calculated from them.

Activity coefficients of both molecules and ions are calculated from electrolyte NRTL model. The excess Gibbs energy of a solution is given by [7]:

$$\frac{G_m^{*E}}{RT} = \frac{G_m^{*E,PDH}}{RT} + \frac{G_m^{*E,Born}}{RT} + \frac{G_m^{*E,Local}}{RT} \tag{4}$$

The first term on the right of Eq. (4) is the long range ion-ion interaction contribution, and the reference state for ionic speciation is the infinite dilute state of electrolyte in the mixed solvent. The third term is the local contribution for short range interactions which is obtained by electrolyte NRTL model, and the reference state for ion is the infinite dilute state in water. To account for the difference of reference state between the two terms, the Born expression is introduced into the excess Gibbs energy equation. Then, the activity coefficients can be derived from the partial derivative of Eq. (4) with respect to the mole number.

The vapor-liquid equilibrium for component i=H_2O, MDEA or PZ:

$$y_i \hat{\varphi}_i^{v} P = \gamma_i x_i \hat{\varphi}_i^{s} P_i^{s} \exp\left[\frac{V_i^{l}(P - P_i^{s})}{RT}\right] \tag{5}$$

and the vapor-liquid equilibrium for CO_2 is given by:

$$y_i \hat{\varphi}_i^{v} P = \gamma_i x_i \left(\frac{H_i}{\gamma_i^{\infty}}\right) \exp\left[\frac{V_i^{\infty,aq}(P - P_{H_2O}^{s})}{RT}\right] \tag{6}$$

where y_i is the true mole fraction in the vapor phase of component i, ϕ_i is the vapor phase fugacity coefficient of component i which is calculated by Redlich-Kwong-Soave equation of state, γ_i is the activity coefficient of component i, P_i^s is the saturation pressure of component i at the system temperature, V_i^l is the molar volume of pure solvent at the system temperature and saturation pressure, γ_i^{∞} is the infinite dilution activity coefficient for CO_2 in solution at the system temperature, $V_i^{\infty,aq}$ is the Brelvi-O'Connell partial molar volume for CO_2 at infinite dilution in H_2O at system temperature and $P_{H_2O}^s$, H_i is the Henry's constant of component i in the mixed solvent, and is calculated by [19]:

$$\ln\frac{H_i}{\gamma_i^{\infty}} = \sum_A W_A \ln\frac{H_{i,A}}{\gamma_{i,A}^{\infty}} \tag{7}$$

where $H_{i,A}$ is the Henry's constant of component i in the solvent A. The value for the MDEA and PZ are fitted to the experimental VLE data of the ternary systems. W_A is calculated by:

$$W_A = \frac{x_A (V_{c,A})^{2/3}}{\sum_B x_B (V_{c,B})^{2/3}} \tag{8}$$

Combining with the mass balance for the components and the condition for liquid-phase electroneutrality, the thermodynamic model is closed and can be solved.

2.2 Model parameters

The interaction parameters of H_2O and molecules in the liquid are taken from literature [20]. Since the volatilities of MDEA and PZ are low, and the gas phase mainly consists of H_2O and CO_2, the binary interaction parameters of SRK are set to zero except the H_2O and CO_2 are taken from literature [20]. The standard properties of protonated and diprotonated piperazine are taken from the literature [19]. Aqueous phase Gibbs free energy, heat of formation and heat capacity at infinite dilution for the quaternary system are listed in Tables 1 and 2, which are used to calculate the reaction equilibrium constants. In addition to the equilibrium

constants, the Henry's constants have significant effect on the solubility behavior. In most of the previous studies, the Henry's constant in the pure water is adopted in the electrolyte system. Since the solubility of gas in electrolyte solutions is affected by the ions and solvents [21,22], it seems more reasonable to apply a revised value. Therefore, the Henry's constants of CO_2 in MDEA and PZ are regressed and used to revise the value in the pure water, as shown in Table 3. Table 4 shows the values of interaction parameters as a function of temperature. It should be note that, introducing more interaction parameters do not always lead to a better agreement between experimental and calculated results. Besides, it should try many times of regression to achieve a satisfied result caused by the strongly nonlinear property and many parameters to be regressed in the fitting process.

3 Results and discussion

Table 5 displays the comparisons between experimental VLE data and model results. For the binary systems of H_2O-MDEA and H_2O-PZ, the calculated values agree well with the experimental data. For the ternary systems, the introduction of CO_2 leads to the increment of reaction and speciation, and model results represent experimental data with reasonable accuracy. It should be noted that, for the H_2O-PZ-CO_2 system, the experimental heat capacity [19] has been added in the regression. To describe the quaternary system, additional parameters are regressed to the work of Pérez-Salado Kamps *et al*. [13], Bottger *et al*. [14] and Speyer *et al*. [15]. The comparisons of correlation and experimental results are shown in Figures 2 to 6. Model results are further compared to the experimental data available in the literatures. The comparisons show that, the model can accurately represent many of the experimental data in a wide range of pressure and temperature. However, there are still some experimental data that cannot be predicted precisely. It mainly results from the following aspects: (1) there is considerable scatter of experimental data both within and between the different data sources; (2) the model has strongly nonlinear property and many parameters to be regressed, which is demanding on the optimization algorithm. In addition, maybe the electrolyte NRTL model should be improved to better describe the complex system.

Measurements and predictions of speciation are imported when modeling kinetic reactions of CO_2 absorption process. The speciation concentration in aqueous solutions of PZ-MDEA-CO_2 was studied by several authors by NMR spectroscopy. Derks *et al*. [9] reported the speciation concentration of the system at 298 K. The spectra give the concentrations of PZ+PZH^++PZH_2^+, $PZCOO^-$+HPZCOO and $PZ(COO^-)_2$. Figure 7 compares the experimental data with model results. The predicted results represent experimental data of PZ+PZH^++PZH_2^+ and $PZCOO^-$+HPZCOO with the AARDs of 12.45 % and 13.13 %. However, the deviation

Table 1 Aqueous phase free energy and heat of formation at infinite dilution and 25 °C

Component	PZH^+ a)	PZH_2^{2+} a)	HPZCOO	$PZCOO^-$	$PZ(COO^-)_2$	$MDEAH^+$
$\Delta_f G_m^{\infty,aq}$ (J/kmol)	1.02×10^8	9.19×10^7	-2.71×10^8	-2.11×10^8	-5.30×10^8	-2.59×10^8
$\Delta_f H_m^{\infty,aq}$ (J/kmol)	-9.15×10^7	-1.23×10^8	-5.39×10^8	-4.60×10^8	1.09×10^8	-5.08×10^8

a) Parameters taken from the literature [19].

Table 2 Aqueous phase heat capacity at infinite dilution a)

Component	*A*	*B*	*C*	*D*
PZH^+ b)	6.04×10^5	-2.52×10^3	4.17	-5.36×10^7
PZH_2^{2+} b)	1.22×10^6	-5.11×10^3	7.07	-1.09×10^8
$PZCOO^-$	15.67	2.32×10^4	−66.26	–
$PZ(COO^-)_2$	-1.20×10^4	−11.91	−436.44	–
HPZCOO	-1.12×10^7	4.55×10^4	−27.29	–
$MDEAH^+$	1.25×10^5	1.15×10^4	−33.45	–

a) $C_p^{\infty,aq} = A + BT + CT^2 + D/T$; b) parameters taken from the literature [19].

Table 3 Henry's constants of CO_2 in solvent a)

Component	*A*	*B*	*C*	*D*	Source
H_2O	170.71	−8477.71	−21.96	5.78×10^{-3}	Chen *et al*. [23]
MDEA	10.35	−4657.55	2.73	–	Regressed
PZ	1.87	−0.65	3.90	–	Regressed

a) $\ln H = A + B/T + C\ln T + DT$.

Table 4 Interaction parameters for the electrolyte NRTL model [a)]

Parameter	*C*	*D*	*E*
	H_2O-MDEA-CO_2		
MDEA-CO_2	–2.259	–748.863	–
CO_2-MDEA	20.084	5467.086	–
($MDEAH^+$,HCO_3^-)-H_2O	–0.398	–536.164	–4.324
H_2O-($MDEAH^+$,HCO_3^-)	–10.101	3875.597	–131.288
($MDEAH^+$,HCO_3^-)-MDEA	23.081	8046.440	389.766
MDEA-($MDEAH^+$,HCO_3^-)	–19.247	6784.904	684.599
($MDEAH^+$,HCO_3^-)-CO_2	–47.069	14551.526	229.745
CO_2-($MDEAH^+$,HCO_3^-)	25.564	–7950.454	–200.490
($MDEAH^+$,CO_3^{2-})-H_2O	–5.988	–1004.962	–
H_2O-($MDEAH^+$,CO_3^{2-})	12.865	–84.140	–
($MDEAH^+$,HCO_3^-)-($MDEAH^+$,CO_3^{2-})	10.671	–10000.000	–
	H_2O-PZ-CO_2		
PZ-CO_2	11.055	–	–
CO_2-PZ	1.440	–	–
(PZH^+,HCO_3^-)-H_2O	–11.936	–17.954	–
H_2O-(PZH^+,HCO_3^-)	16.917	–25.376	–
(PZH^+,$PZCOO^-$)-H_2O	–7.062	–21.344	–
H_2O-(PZH^+,$PZCOO^-$)	15.367	–	–
(PZH^+,HCO_3^-)-CO_2	3.397	–	–
CO_2-(PZH^+,HCO_3^-)	–2.536	–	–
(PZH^+,$PZCOO^-$)-CO_2	–0.958	–	–
CO_2-(PZH^+,$PZCOO^-$)	7.005	–	–
(PZH^+,HCO_3^-)-PZ	–6.403	–11.673	–
PZ-(PZH^+,HCO_3^-)	0.652	–	–
(PZH^+,$PZCOO^-$)-PZ	0.814	–	–
PZ-(PZH^+,$PZCOO^-$)	21.293	–	–
(PZH^+,HCO_3^-)-(PZH^+,$PZCOO^-$)	–8.224	–	–
(PZH^+,$PZCOO^-$)-(PZH^+,HCO_3^-)	21.732	–	–
	H_2O-MDEA-PZ-CO_2		
PZ-MDEA	–1.576	–	–0.272
MDEA-PZ	–7.054	–26.367	0.093
($MDEAH^+$,$PZCOO^-$)-H_2O	28.012	–252.556	13.011
H_2O-($MDEAH^+$,$PZCOO^-$)	4.142	–35.888	0.850
(PZH^+,HCO_3^-)-MDEA	21.520	184.627	–12.941
MDEA-(PZH^+,HCO_3^-)	27.220	–80.530	–14.107
($MDEAH^+$,HCO_3^-)-PZ	38.631	205.096	25.102
PZ-($MDEAH^+$,HCO_3^-)	161.384	–663.360	–3.850
(PZH^+,$PZCOO^-$)-MDEA	0.207	–	–
MDEA-(PZH^+,$PZCOO^-$)	–1.470	–	–
($MDEAH^+$,$PZCOO^-$)-PZ	–0.304	–15.469	–
PZ-($MDEAH^+$,$PZCOO^-$)	–3.549	–	–
($MDEAH^+$,$PZCOO^-$)-CO_2	0.022	21.330	–
CO_2-($MDEAH^+$,$PZCOO^-$)	–0.807	3.962	–
MDEA-($MDEAH^+$,$PZCOO^-$)	–0.528	9.502	–
($MDEAH^+$,$PZ(COO^-)_2$)-H_2O	–2.227	76.092	–
H_2O-($MDEAH^+$,$PZ(COO^-)_2$)	–1.127	7.255	–
($MDEAH^+$,CO_3^{2-})-PZ	–12.283	–	–
PZ-($MDEAH^+$,CO_3^{2-})	–0.908	–	–
(PZH^+,CO_3^{2-})-MDEA	2.765	–	–
MDEA-(PZH^+,CO_3^{2-})	1.620	–	–

a) For the molecule-molecule: $\tau=C+D/T+E\ln T$; for the molecule-salt, salt-molecule and salt-salt: $\tau=C+D/T+E[(T^{ref}-T)/T+\ln(T/T^{ref})]$.

Table 5 Comparison between experimental VLE data from the literatures and model results

Source	N [b]	Experimental ranges						AARD [a]	
		T (K)	m_{MDEA} (mol/kg) [c]	m_{PZ} (mol/kg) [c]	m_{CO_2} (mol/kg) [c]	P_{CO_2} (kPa)	P (kPa)	$\left\|\frac{\Delta P_{CO_2}}{P_{CO_2}}\right\|$ (%)	$\left\|\frac{\Delta P}{P}\right\|$ (%)
H_2O-MDEA									
[24]	34	326–381	0.9–20	–	–	–	13–102	–	2.20
[25]	27	350–459	3.6–774	–	–	–	40–67	–	3.98
[26]	61	313–373	0–31	–	–	–	6–100	–	1.70
H_2O-PZ									
[19]	46	305–337	–	0.9–5	–	–	5.0–23	–	5.10
[13]	2	393	–	2.0–4	–	–	180–200	–	2.21
H_2O-MDEA-CO_2									
[27]	63	373–473	2.1–8.0	–	0.05–4.1	103–4930	–	28.75	–
[28]	5	313	2.6	–	0.3–3.2	1.2–3770	–	24.32	–
[29] [d]	82	313–413	1.95–4	–	0–4.6	–	73–5037	–	7.73
[30] [d]	28	313–393	3.9–8	–	1–9.3	–	176–7565	–	14.2
[31] [d]	101	313–393	1.9–8.4	–	0.018–4.7	0.12–69.3	–	12.41	–
[32]	103	298–348	2.9–7.4	–	0–8.2	–	2.7–4560	–	10.20
[33]	34	328–358	8.4	–	1.4–6.8	66–813	–	13.41	–
[34]	12	373–393	8.5	–	0.7–7	160–3900	–	15.04	–
[35]	118	298–393	2.6–8.5	–	0–11.0	0–6630	–	57.08	–
[36]	37	313–373	4.5	–	0–3.6	0–262	–	27.51	–
H_2O-PZ-CO_2									
[13] [d]	94	313–393	–	2.0–4.0	0–5.4	–	13–9560	–	14.88
[19] [d]	62	313–333	–	0.9–5.2	0.2–4.1	0.02–51	–	32.16	–
[37]	52	313–393	–	0.9–4.5	0.2–3.4	0.1–95.3	–	15.55	–
[38]	16	313–343	–	0.65	0.1–0.6	0.03–40	–	17.68	–
[39]	42	313–343	–	0.3–1.4	0.3–2.9	198–7399	–	41.14	–
[40]	36	393–423	–	4.7–11.3	2.2–7.3	77–2234	–	29.73	–
[41]	43	313–373	–	2.0–12.0	0.9–8.5	0.06–39.3	–	44.52	–
H_2O-MDEA-PZ-CO_2									
[1]	80	303–363	1.6–12	0.2–4	0.7–10	13–935	–	28.90	–
[13] [d]	10	353	1.98	1.97	2.5–4.5	–	181–6400	–	10.73
[14] [d]	71	313–393	2.2–7.8	≈2.0	1.9–11	–	218–11880	–	17.04
[15] [d]	151	313–393	2.0–8.5	1.0–4.0	0.1–6.1	0.1–147	–	16.53	–
[11]	82	313–343	3.0–5.0	0.6–2.3	1.2–7.6	27–3938	–	36.43	–
[12]	18	363	2.0–5.0	0.4–1.0	0.7–2	27–204	–	28.77	–
[42]	27	313–353	1.8–2	0.01–0.1	0.1–2	0.06–96	–	19.72	–
[9]	20	313	8.6	1.3	1.2–6.3	0.70–90	–	12.35	–
[9]	64	298–323	0.6–4.8	1.2–2	0.7–5	0.20–110	–	39.20	–
[43]	10	343	8.7–9.7	0.2–1.2	0.4–2.8	7–83	–	18.57	–
[17]	13	313–343	8.6	1.3	0.02–1.3	0.03–7.5	–	24.79	–
[44]	19	313–433	7	2	0.2–2.6	0.19–2452	–	27.20	–
[44]	20	313–433	5	5	1.8–3.7	0.24–1746	–	28.11	–

a) Average absolute relative deviations; b) number of data points; c) m is molality, mol/(kg water); d) experimental data used to regression.

for the $PZ(COO^-)_2$ is relatively large, which may partly result from the experimental uncertainty, because of the low concentration of $PZ(COO^-)_2$ in the solutions.

Bottinger *et al*. [45] reported experimental results of speciation concentration in the quaternary system at different temperatures and mass concentrations of PZ and MDEA. Comparisons of experimental and model results are shown in Figures 8 to 10. The AARDs for the MDEA+$MDEAH^+$ are 2.79% (at 293.15 K), 3.92% (at 313.15 K) and 3.28% (at 333.15 K). Model results agree well with the experimental data. For the PZ+PZH^++PZH_2^+, the values are 29.62 % (at 298.15 K), 42.27% (at 313.15 K) and 38.43% (at 333.15 K). The differences between experimental and predicted results for the $PZCOO^-$+HPZCOO are 39.63% (at 298.15 K), 32.54% (at 313.15 K, with the exception of a single data point) and 28.73% (at 333.15 K). Model results can describe the trends of experimental data. Since there are zero value for the experimental concentrations of PZ $(COO^-)_2$ and HCO_3^-+CO_3^{2-}, the AARDs for the speciation are not given explicitly here. The difference between predicted and experimental results may result from the following two aspects. First, the experimental uncertainty for the speciation

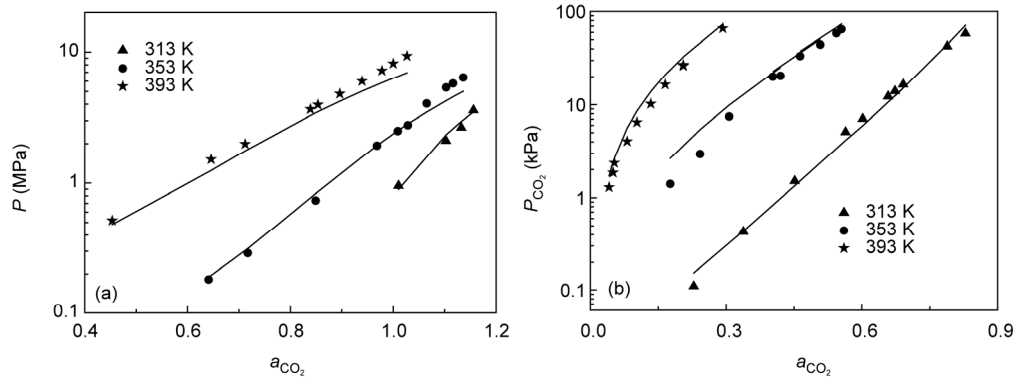

Figure 2 Total pressure (a) and partial pressure (b) of H_2O-MDEA-PZ-CO_2. $m_{MDEA} \approx 2$ mol/kg, $m_{PZ} \approx 2$ mol/kg. Symbols are experimental data from reference [13–15], lines are model results. a_{CO_2} is CO_2 loading, mol CO_2/(mol amine).

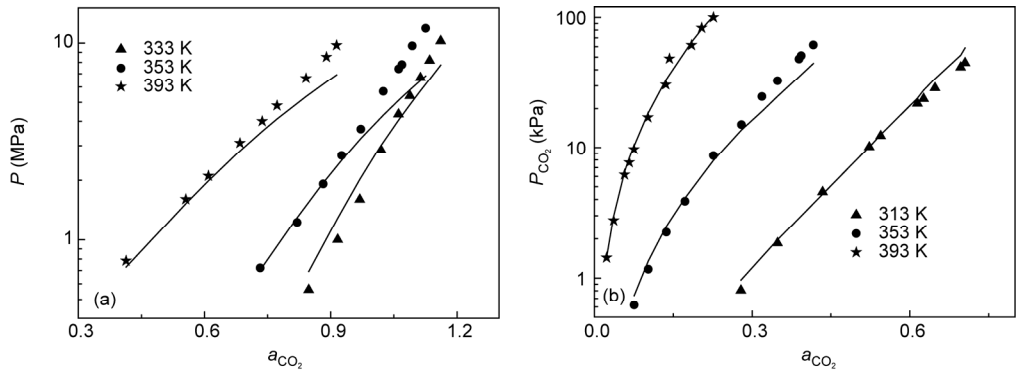

Figure 3 Total pressure (a) and partial pressure (b) of H_2O-MDEA-PZ-CO_2. $m_{MDEA} \approx 4$ mol/kg, $m_{PZ} \approx 2$ mol/kg. Symbols are experimental data from reference [14,15], lines are model results.

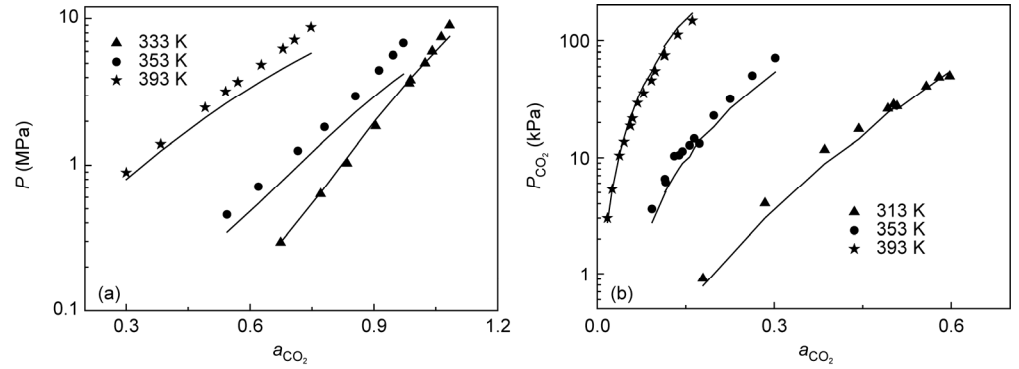

Figure 4 Total pressure (a) and partial pressure (b) of H_2O-MDEA-PZ-CO_2. $m_{MDEA} \approx 8$ mol/kg, $m_{PZ} \approx 2$ mol/kg. Symbols are experimental data from reference [14,15], lines are model results.

with low concentration is comparatively large. Second, there are byproducts in the solutions which are not considered in the model.

Heat of absorption is an important parameter for the design of equipment and process. Svensson *et al*. [46] reported the integral and differential heat of CO_2 absorption in the aqueous solution of PZ and MDEA at the temperature from 308.15 to 338.15 K. In the model, the integral heat is calculated from the enthalpy balance of an absorption process [47]. The differential heat is calculated by [48]:

$$-\frac{\Delta H_{abs}}{R} = \frac{\mathrm{d}\ln f_{CO_2}}{\mathrm{d}(1/T)} \tag{9}$$

where f is the fugacity. Table 6 shows the comparison of experimental and model results. Apart from several outliers, model results are in reasonable agreement with the experimental data. To better represent the heat of absorption, ex-

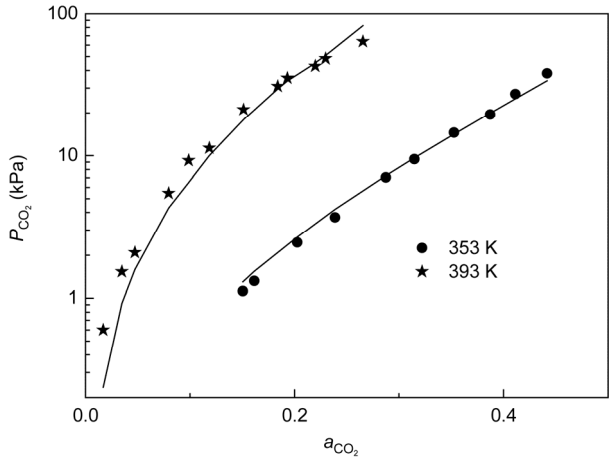

Figure 5 Partial pressure of H_2O-MDEA-PZ-CO_2 . $m_{MDEA} \approx 4$ mol/kg, $m_{PZ} \approx 4$ mol/kg. Symbols are experimental data from reference [15], lines are model results.

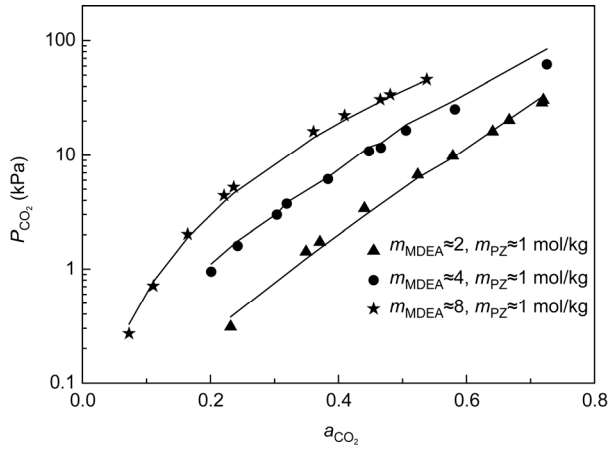

Figure 6 Partial pressure of H_2O-MDEA-PZ-CO_2 at T=313 K. Symbols are experimental data from reference [15], lines are model results.

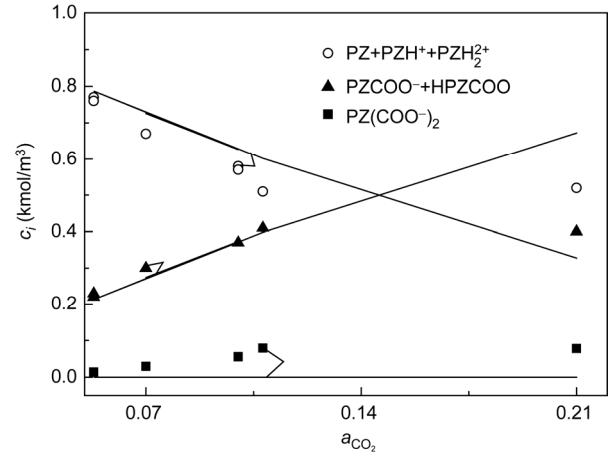

Figure 7 Speciation in the mixture of H_2O-PZ-MDEA-CO_2 at T=298.15 K (C_{MDEA}=4.0 kmol/m^3, C_{PZ}=1.0 kmol/m^3). Symbols represent experimental results from Derks *et al*. [9]; lines represent the model results.

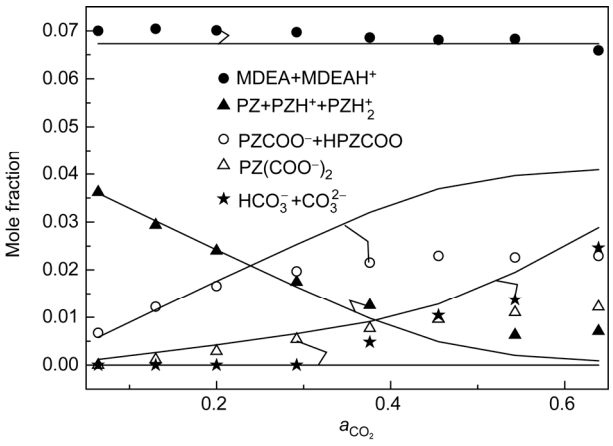

Figure 8 Speciation in mixture of H_2O-PZ-MDEA-CO_2 at T=293.15 K (w_{MDEA}=0.29, w_{PZ}=0.13). Symbols represent experimental results from Bottinger *et al*. [45]; lines represent the model results.

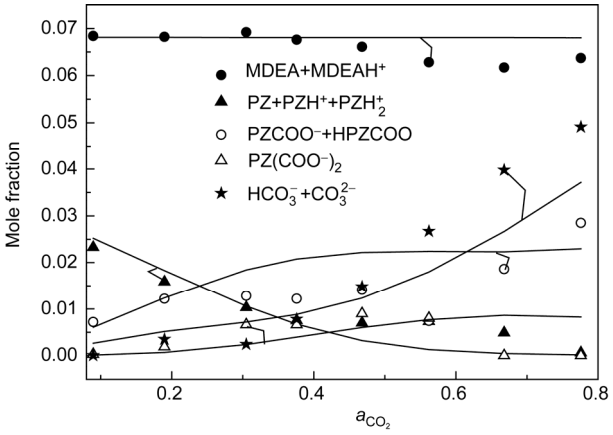

Figure 9 Speciation in mixture of H_2O-PZ-MDEA-CO_2 at T=313.15 K (w_{MDEA}=0.3, w_{PZ}=0.1). Symbols represent experimental results from Bottinger *et al*. [45]; lines represent the model results.

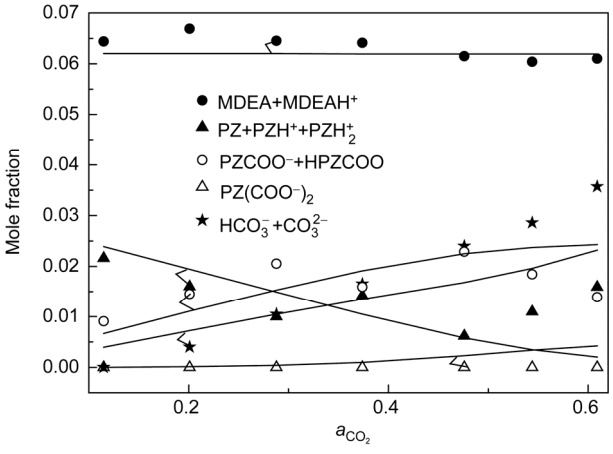

Figure 10 Speciation in mixture of H_2O-PZ-MDEA-CO_2 at T=333.15 K (w_{MDEA}=0.28, w_{PZ}=0.1). Symbols represent experimental results from Bottinger *et al*. [45]; lines represent the model results.

Table 6 Comparison of experimental and model results of heat of absorption (w_{MDEA}=0.2, w_{PZ}=0.05)

T (K)	a_{CO2}	$\Delta H_{int,exp}$ (kJ/mol) [a]	$\Delta H_{int,cal}$	ARD	$\Delta H_{diff,exp}$ [b]	$\Delta H_{diff,cal}$	ARD [c]
	0.045	76.7	79.94	0.042	76.7	81.25	0.059
	0.11	83.3	72.76	0.127	87.9	85.79	0.024
	0.209	78.7	66.46	0.156	73.6	86.48	0.175
308.15	0.047	83.8	79.63	0.050	83.8	81.41	0.029
	0.126	78.9	71.57	0.093	76.1	86.49	0.136
	0.235	74.6	65.05	0.128	69.7	86.96	0.248
	0.37	70	58.08	0.170	62	87.16	0.406
	0.045	82.4	81.37	0.013	82.4	79.64	0.033
	0.117	81.8	60.65	0.259	81.3	88.01	0.083
	0.221	78.2	39.96	0.489	74.2	60.37	0.186
318.15	0.048	80.3	80.24	0.001	80.3	80.72	0.005
	0.131	78.6	57.43	0.269	77.6	86.32	0.112
	0.24	76.3	36.93	0.516	73.4	54.48	0.258
	0.376	72.2	20.34	0.718	64.9	29.36	0.548
	0.041	84.2	85.18	0.012	84.2	60.92	0.276
	0.111	83.3	77.89	0.065	82.8	50.44	0.391
	0.206	80.4	80.57	0.002	77	41.65	0.459
328.15	0.044	84.5	84.42	0.001	84.5	61.07	0.277
	0.115	83.9	77.81	0.073	83.5	49.66	0.405
	0.216	79.4	81.29	0.024	74.3	42.55	0.427
	0.345	75.2	92.35	0.228	68.2	69.23	0.015
	0.035	88.2	81.50	0.076	88.2	56.02	0.365
	0.098	86.1	68.30	0.207	84.9	63.32	0.254
	0.191	82.1	61.70	0.248	78	66.24	0.151
338.15	0.043	82.9	78.41	0.054	82.9	57.60	0.305
	0.111	82.7	67.03	0.190	82.5	64.11	0.223
	0.206	80.3	60.97	0.241	77.4	66.43	0.142
	0.325	77.3	56.26	0.272	72.1	65.70	0.089

a) Integral heat of CO_2 absorption, kJ/(mol CO_2); b) differential heat of CO_2 absorption, kJ/(mol CO_2); c) absolute relative deviations.

perimental data can be added into the regression process.

4 Conclusions

Aqueous solution of PZ and MDEA is widely used to remove carbon dioxide from natural gas or gaseous effluents. The knowledge of solubility behavior is essential to the design and optimization of equipment and process. In the work, the phase and chemical equilibriums of the quaternary system are studied by electrolyte NRTL model. In the model, the chemical equilibrium constants are calculated from the standard Gibbs free energy of formation, the enthalpy of formation and the heat capacity. In addition, the Henry's constants of CO_2 in amines are regressed to revise the value in the pure water. The model increases the degree of freedom of the phase and chemical equilibrium constants which is beneficial to accurately describe the solubility behavior in different temperature conditions. Model results represent the experimental VLE, NMR spectroscopy and heat of absorption data with reasonable accuracy. Furthermore, since new experimental data with wider ranges have been added to the regression, the model should provide a comprehensive thermodynamic representation for the quaternary system with broader ranges and more accurate predictions than previous work. However, the model has strongly nonlinear property and many parameters to be regressed, much work needs to be done to obtain the satisfactory regression result.

Acknowledgments This work was supported by the National Natural Science Foundation of China (51376188), and the National Basic Research Program of China (2011CB710701).

Conflict of interest The authors declare that they have no conflict of interest.

1 Liu HB, Zhang CF, Xu GW. *Ind Eng Chem Res*, 1999, 38: 4032–4036
2 Zhang SJ, Zhang XP, Zhao YS, Zhao GY, Yao XQ, Yao HW. *Sci China Chem*, 2010, 53: 1549–1553
3 Kent RL, Eisenberg B. *Hydrocarbon Process Int Ed*, 1976, 55: 87–90
4 Tontiwachwuthikul P, Meisen A, Lim CJ. *J Chem Eng Data*, 1991, 36: 130–133
5 Posey ML, Tapperson KG, Rochelle GT. *Gas Sep Purif*, 1996, 10: 181–186
6 Leung KS, Chan SWK, Wong WSF, Gullett EA, Buttenham S, Hore T, Haji-Sulaiman MZ, A roua MK, Pervez MI. *Gas Sep Purif*, 1996, 10: 13–18
7 Austgen DM, Rochelle GT, Peng X, Chen CC. *Ind Eng Chem Res*, 1989, 28: 1060–1073
8 Li C, Fürst W. *Chem Eng Sci*, 2000, 55: 2975–2988
9 Derks PWJ, Hogendoorn JA, Versteeg GF. *J Chem Thermodyn*, 2010, 42: 151–163

10 Deshmukh RD, Mather AE. *Chem Eng Sci*, 1981, 36: 355–362
11 Vahidi M, Matin NS, Goharrokhi M, Jenab MH, Abdi MA, Najibi SH. *J Chem Thermodyn*, 2009, 41: 1272–1278
12 Najibi H, Maleki N. *Fluid Phase Equilib*, 2013, 354: 298–303
13 Pérez-Salado Kamps Á, Xia J, Maurer G. *AlChE J*, 2003, 49: 2662–2670
14 Bottger A, Ermatchkov V, Maurer G. *J Chem Eng Data*, 2009, 54: 1905–1909
15 Speyer D, Ermatchkov V, Maurer G. *J Chem Eng Data*, 2009, 55: 283–290
16 Ermatchkov V, Maurer G. *Fluid Phase Equilib*, 2011, 302: 338–346
17 Bishnoi S. *Carbon Dioxide Absorption and Solution Equillibrium in Piperazine Activated Methyldiethanolanine Dissertation of Doctoral Degree*. Texas: University of Texas at Austin, 2001
18 Pinto DDD, Monteiro JGMS, Bersås A, Haug-Warberg T, Svendsen HF. *Energy Procedia*, 2013, 37: 1613–1620
19 Hilliard MD. A predictive thermodynamic model for an aqueous blend of potassium carbonate, piperazine, and monoethanolamine for carbon dioxide capture from flue gas. *Dissertation of Doctoral Degree*. Texas: University of Texas at Austin, 2008
20 Aspen Physical Property System, V7.2; Burlington, MA: Aspen Technology, Inc., 2010
21 Joosten GEH, Danckwerts PV. *J Chem Eng Data*, 1972, 17: 452–454
22 Zhang Y, Que H, Chen CC. *Fluid Phase Equilib*, 2011, 311: 67–75
23 Chen CC, Britt HI, Boston JF, Evans LB. *AlChE J*, 1979, 25: 820–831
24 Xu S, Qing S, Zhen Z, Zhang C. *Fluid Phase Equilib*, 1991, 67: 197–201
25 Voutsas E, Vrachnos A, Magoulas K. *Fluid Phase Equilib*, 2004, 224: 193–197
26 Kim I, Svendsen HF, Børresen E. *J Chem Eng Data*, 2008, 53: 2521–2531
27 Chakma A, Meisen A. *Ind Eng Chem Res*, 1987, 26: 2461–2466
28 Macgregor RJ, Mather AE. *Can J Chem Eng*, 1991, 69: 1357–1366
29 Kuranov G, Rumpf B, Smirnova NA, Maurer G. *Ind Eng Chem Res*, 1996, 35: 1959–1966
30 Kamps ÁPS, Balaban A, Jödecke M, Kuranov G, Smirnova NA, Maurer G. *Ind Eng Chem Res*, 2001, 40: 696–706
31 Ermatchkov V, Kamps ÁPS, Maurer G. *Ind Eng Chem Res*, 2006, 45: 6081–6091
32 Sidi-Boumedine R, Horstmann S, Fischer K, Provost E, Furst W, Gmehling J. *Fluid Phase Equilib*, 2004, 218: 85–94
33 Ma'mun S, Nilsen R, Svendsen HF, Juliussen O. *J Chem Eng Data*, 2005, 50: 630–634
34 Dawodu OF, Meisen A. *J Chem Eng Data*, 1994, 39: 548–552
35 Jou FY, Mather AE, Otto FD. *Ind Eng Chem Proc Des Dev*, 1982, 21: 539–544
36 Jou FY, Carroll JJ, Mather AE, Otto FD. *Can J Chem Eng*, 1993, 71: 264–268
37 Ermatchkov V, Kamps ÁPS, Speyer D, Maurer G. *J Chem Eng Data*, 2006, 51: 1788–1796
38 Bishnoi S, Rochelle GT. *Chem Eng Sci*, 2000, 55: 5531–5543
39 Kadiwala S, Rayer AV, Henni A. *Fluid Phase Equilib*, 2010, 292: 20–28
40 Xu Q. Thermodynamics of CO_2 loaded aqueous amines. *Dissertation of Doctoral Degree*. Texas: University of Texas at Austin, 2011
41 Dugas RE, Rochelle GT. *J Chem Eng Data*, 2011, 56: 2187–2195
42 Ali BS, Aroua MK. *Int J Thermophys*, 2004, 25: 1863–1870
43 Xu GW, Zhang CF, Qin SJ, Gao WH, Liu HB. *Ind Eng Chem Res*, 1998, 37: 1473–1477
44 Nguyen T. Amine volatility in CO_2 capture. *Dissertation of Doctoral Degree*. Texas: University of Texas at Austin, 2013
45 Bottinger W, Maiwald M, Hasse H. *Ind Eng Chem Res*, 2008, 47: 7917–7926
46 Svensson H, Hulteberg C, Karlsson HT. *Int J Greenh Gas Con*, 2013, 17: 89–98
47 Zhang Y, Chen CC. *Ind Eng Chem Res*, 2010, 50: 163–175
48 Frailie P, Plaza J, van Wagener D, Rochelle GT. *Energy Procedia*, 2011, 4: 35–42